Nuclear Physics B225 [FS9] (1983) 156–168

WILSON LOOPS FOR U(4) AND SU(4) LATTICE GAUGE THEORIES IN FOUR DIMENSIONS

D. BARKAI

Center for Applied Vector Technology, Control Data Corporation at the Institute for Computational Studies, Colorado State University, Fort Collins, Colorado 80523, USA

Michael CREUTZ

Brookhaven National Laboratory, Upton, New York 11973, USA

K.J.M. MORIARTY

CERN, Geneva, Switzerland

Received 6 December 1982
(Revised 28 February 1983)

Monte Carlo simulations are used to calculate Wilson loops for pure U(4) and SU(4) gauge theories on a 6^4 lattice. The first-order phase transitions previously observed in the average action per plaquette for U(4) and SU(4) is also seen in the string tension. U(4) and SU(4) color seem to be confined while U(1) charge in U(4) appears to be deconfined.

In previous studies, we examined pure U(4) [1] and SU(4) [2] lattice gauge theories in four space–time dimensions. Since first-order phase transitions were found in both of these theories, it seems reasonable that these theories should be studied together so that they can be compared and contrasted. To make a more detailed exploration of the phase transitions in these theories, we study the string tensions, via the Wilson loops, for these gauge groups. The decoupling of the SU(4) and U(1) components of the U(4) gauge group, in the low-temperature region, should be observed so that U(4) and SU(4) gauge theories should merely be shifted in the inverse temperature. Both U(4) and SU(4) color should be confined while the U(1) charges of U(4) gauge theory should be deconfined. Similar behavior has recently been observed for the gauge groups U(2) [3], SU(2) [4], U(3) [5] and SU(3) [6].

The partition function for the U(N) and SU(N) non-abelian gauge theories on a four-dimensional euclidean lattice is defined by

$$Z(\beta) = \int \left(\prod_{r,\hat{\mu}} \mathrm{d}U_{\hat{\mu}}(r) \right) \exp\left(-\beta S[U]\right),$$

where $U_{\hat{\mu}}(r)$ is an $N \times N$ matrix of the U(N) or SU(N) gauge groups attached to a given link of the lattice identified by the indices r and $\hat{\mu}$ which label the lattice

sites and the unit vectors in the four euclidean directions, respectively. The inverse temperature β is defined by $\beta = 2N/g_0^2$ where g_0 is the bare coupling constant and the measure in the above integral is the invariant Haar measure for the relevant gauge group under consideration. The Wilson action [7] S is defined as a sum over the individual plaquette actions by

$$S[U] = \sum_{\square} S_{\square} = \sum_{r,\hat{\mu}>\hat{\nu}} \left(1 - \frac{1}{N} \operatorname{Re} \operatorname{Tr} \left(U_{r,\hat{\mu}} U_{r+\hat{\mu},\hat{\nu}} U_{r+\hat{\mu}+\hat{\nu},-\hat{\mu}} U_{r+\hat{\nu},-\hat{\nu}}\right)\right),$$

where the trace is analogous to the curl of the continuum theory gauge field A_μ^α where

$$U_{r,\hat{\mu}} = \exp\left(i g_0 A_\mu^\alpha T^\alpha\right),$$

where T^α are U(N) or SU(N) generators. Periodic boundary conditions are used throughout our calculations and the method of Metropolis et al. [8, 9] was used to equilibrate our lattice. A more detailed description of our calculational techniques can be found in ref. [10]. We now examine the particular cases of $N = 4$, i.e. U(4) and SU(4).

The expectation value

$$W(I, J) = \tfrac{1}{4}\langle \operatorname{Re} \operatorname{Tr} U_C \rangle,$$

where C is a rectangular loop of length I and width J and U_C is the product of link variables around the contour C, defines the Wilson loop [7]. The leading-order high-temperature expansion for the U(4) and SU(4) Wilson loops is

$$W(I, J) = \left(\tfrac{1}{32}\beta + \mathrm{O}(\beta^2)\right)^{IJ}, \tag{1}$$

and the leading-order, low-temperature expansions for the average action per plaquette for U(4) and SU(4) are

$$\langle E \rangle = 1 - W(1, 1) = \frac{4}{\beta} + \mathrm{O}(\beta^{-2}), \tag{2}$$

$$\langle E \rangle = 1 - W(1, 1) = \frac{15}{4\beta} + \mathrm{O}(\beta^{-2}), \tag{3}$$

respectively.

For large Wilson loops, we expect the behavior

$$W \sim \exp\left(-A - K \cdot \text{area} - C \cdot \text{perimeter}\right),$$

where the coefficients A, K and C are constants for a given value of the inverse temperature β. When this behavior applies, we extract the string tension K from the logarithmic ratio

$$\chi(I, J) = -\ln \frac{W(I, J) W(I-1, J-1)}{W(I, J-1) W(I-1, J)}.$$

The leading-order high-temperature expansion for the string tension for the U(4) and SU(4) gauge groups is given by

$$\chi(I,J) = -\ln\left(\tfrac{1}{32}\beta\right) + O(\beta^2)\,. \tag{4}$$

The U(1) component of U(4) is obtained by calculating the determinant [11] for each Wilson loop considered as a 4×4 matrix in U(4) and then taking the average over all Wilson loops in the lattice to give the mean indicated by

$$\bar{W}(I,J) = \langle \det(U_C)\rangle\,.$$

From these quantities we form the new logarithmic ratio

$$\bar{\chi}(I,J) = -\ln\frac{\bar{W}(I,J)\bar{W}(I-1,J-1)}{\bar{W}(I,J-1)\bar{W}(I-1,J)}\,.$$

The leading-order high-temperature expansion for the average determinants for U(4) is

$$\bar{W}(I,J) = \left[\tfrac{1}{98308}\beta^4 + O(\beta^6)\right]^{IJ}, \tag{5}$$

while for the quantity $\bar{\chi}(I,J)$ is

$$\bar{\chi}(I,J) = -\ln\left(\tfrac{1}{98308}\beta^4\right) + O(\beta^6)\,. \tag{6}$$

Of course, for SU(4) the determinant of the 4×4 matrices is identically equal to one.

To obtain our results, we first performed 100 iterations through the lattice with 20 Monte Carlo upgrades per link. Outside a small region in the vicinity of the first-order phase transition, this equilibrated our lattice. We then averaged over the next 50 iterations through the lattice. For these calculations, we used the CRAY-1S with the algorithm described in ref. [10]. In the vicinity of the phase transitions, we performed 200 iterations through the lattice with 20 Monte Carlo updates per link which equilibrated the lattice. We then performed an average over the next 100 iterations through the lattice. This part of the calculation was performed on the CDC CYBER 205 using the red–black vector algorithm, described in ref. [12].

For U(4), we used disordered starts for $\beta \leq 11$, mixed phase starts [13] for $11.0 < \beta \leq 13.0$ and ordered starts for $13.0 < \beta \leq 25.0$. For the mixed phase starts, the fourth axis of the euclidean lattice, the time axis, was divided in two with the upper half of the link variables disordered and the lower half ordered. The runs for $11.9 \leq \beta \leq 13.0$ corresponded to the 300 iterations through the lattice while all others corresponded to the 150 iterations through the lattice. For SU(4), we used disordered starts for $\beta \leq 9.0$, mixed phase starts for $9.0 < \beta \leq 12.0$ and ordered starts for $12.0 < \beta \leq 25.0$. The runs for $10.0 \leq \beta \leq 11.0$ corresponded to the 300 iterations through the lattice. All other calculations corresponded to 150 iterations through the lattice. We checked our calculation by carrying out for each and every value of β, 800 iterations through the lattice, with an average over the last 300

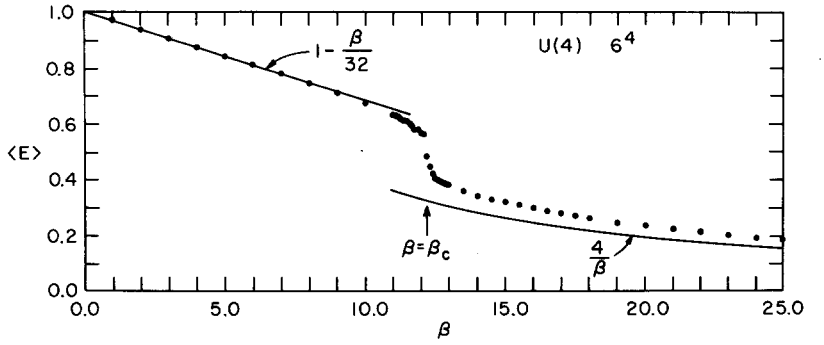

Fig. 1. The average action per plaquette $\langle E \rangle$ for pure U(4) gauge theory on a 6^4 lattice as a function of the inverse temperature β. The curves represent the leading-order high- and low-temperature expansions of eqs. (1) and (2), respectively.

iterations, for only the average action per plaquette. By this means, we located the transition inverse temperature for SU(4) at $\beta_c = 10.205 \pm 0.010$.

We show the average action per plaquette $\langle E \rangle$ for pure U(4) gauge theory as a function of the inverse temperature β on a 6^4 lattice in fig. 1. The leading-order high- and low-temperature expansions of eqs. (1) and (2), respectively, are also shown. Some mixed phase runs for the average action per plaquette in the vicinity of the transition inverse temperature are shown in fig. 2. The first-order phase transition is clearly visible at the inverse temperature of $\beta_c = 12.2 \pm 0.2$. In fig. 3 we present the Wilson loops of size up to 3×3 along with the leading-order high-temperature expansion of eq. (1) which provides a good description of the Monte Carlo data.

The quantity $\chi(I, J)$, for $(I, J) = (1, 1), (2, 2), (3, 2)$ and $(3, 3)$, as a function of the inverse temperature β, is shown in fig. 4a. The leading-order high-temperature expansion of eq. (4) is also presented in fig. 4a and agrees well with the Monte

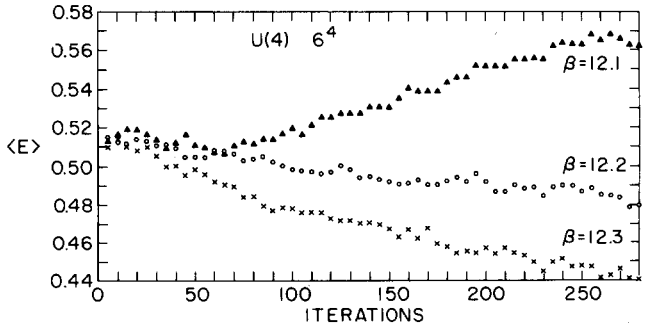

Fig. 2. The evolution of the average action per plaquette $\langle E \rangle$ for pure U(4) gauge theory on a 6^4 lattice as a function of the number of iterations through the lattice for mixed phase starting lattices for various values of the inverse temperature β.

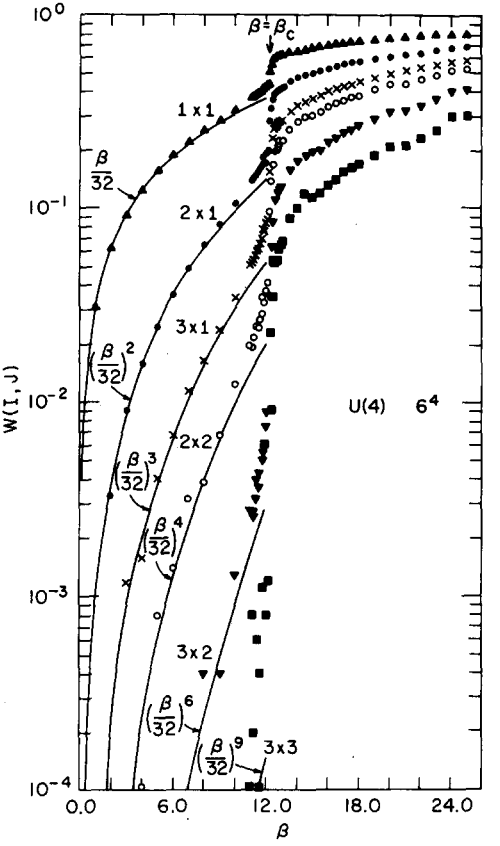

Fig. 3. The Wilson loops $W(I, J)$ for pure U(4) gauge theory on a 6^4 lattice as a function of the inverse temperature β. The full upward triangles represent $(I, J) = (1, 1)$, the full circles represent (2, 1), the crosses represent (2, 2), the full downward triangles represent (3, 2) and the full squares represent (3, 3). The curves represent the leading-order high-temperature expansion of eq. (1).

Carlo data for $\beta < 9.0$. An expanded view of the Monte Carlo data near the transition inverse temperature is shown in fig. 4b. The discontinuous nature of the transition appears enhanced in the larger loop ratios.

At low temperature the U(1) and SU(4) parts of our U(4) matrices should decouple and we are effectively left with an SU(4) theory. The logarithmic ratios for both U(4) and SU(4) are shown in fig. 5. The weak-coupling U(4) results imitate the SU(4) results with the U(4) results simply shifted by approximately 2 units in β.

We show the average U(1) action per plaquette $\langle \bar{E} \rangle = 1 - \bar{W}(1, 1)$ as a function of the inverse temperature β on a 6^4 lattice, in fig. 6. Also presented in fig. 6 is the leading-order high-temperature expansion of eq. (5). Some mixed phase starting runs for $\langle \bar{E} \rangle$ near the transition inverse temperature are shown in fig. 7. From

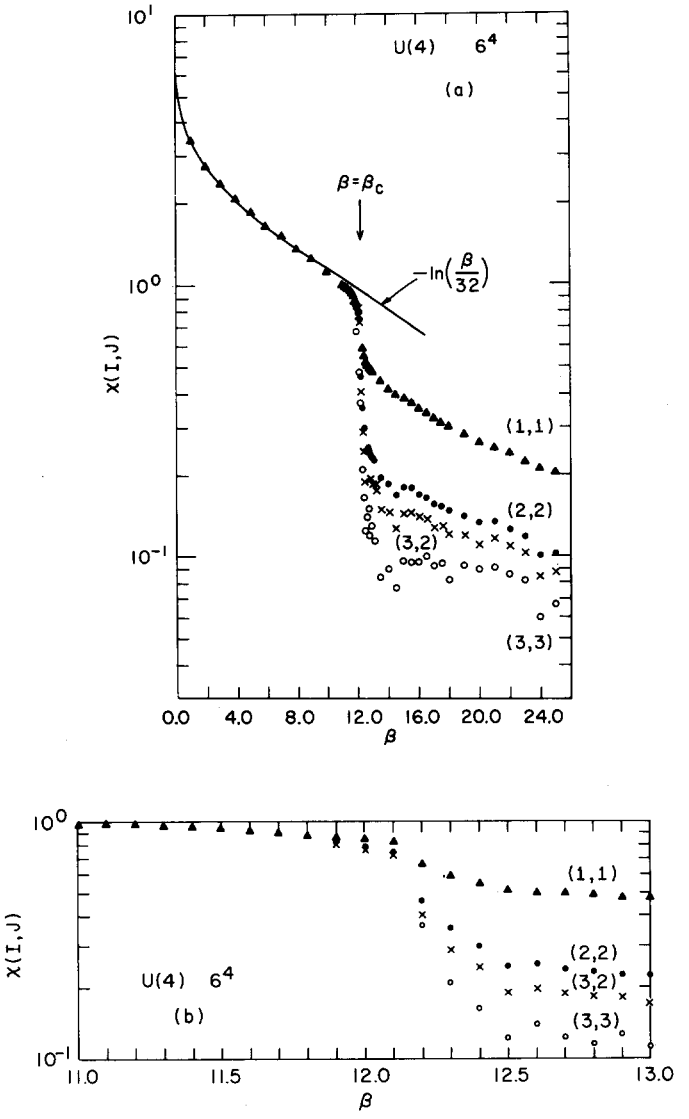

Fig. 4. The logarithmic ratio $\chi(I, J)$ for pure U(4) gauge theory on a 6^4 lattice as a function of the inverse temperature β. The full upward triangles represent $(I, J) = (1, 1)$, the full circles represent (2, 2), the crosses represent (3, 2) and the open circles represent (3, 3). Also shown in the diagram is the leading-order high-temperature expansion of eq. (4).

these diagrams, the phase transition would appear to be of first order which is in contrast with the second-order phase transition previously found in pure U(1) gauge theory [14]. In fig. 8 we show the results for the U(1) Wilson loops $\bar{W}(I, J)$ of size up to 3×3 along with eq. (5) for comparison.

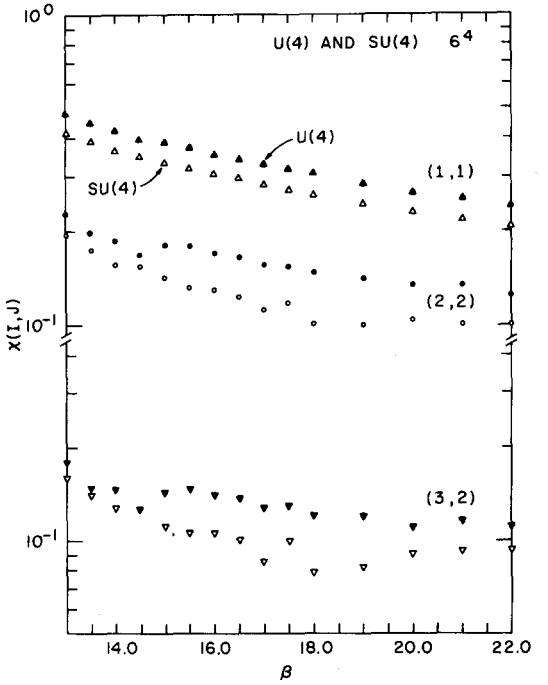

Fig. 5. A comparison of the string tension $\chi(I, J)$ as a function of the inverse temperature β for pure U(4) and SU(4) gauge theories on 6^4 lattices. The full (open) upward triangles represent $(I, J) = (1, 1)$, the full (open) circles represent (2, 2) and the full (open) downward triangles represent (3, 2) for U(4) and SU(4), respectively.

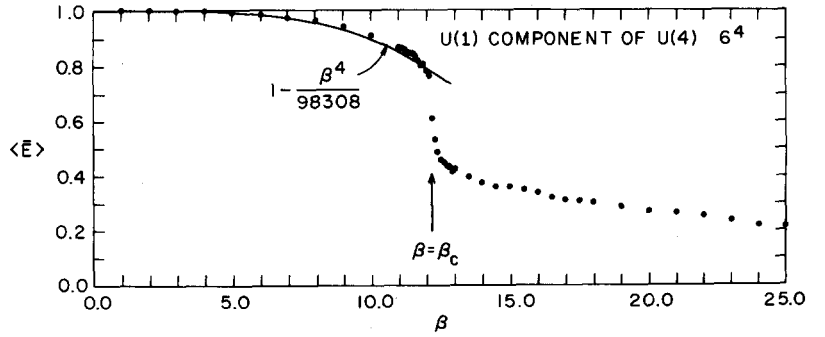

Fig. 6. The average U(1) action per plaquette $\langle\bar{E}\rangle$ on a 6^4 lattice as a function of the inverse temperature β. The curve represents the leading-order high-temperature expansion of eq. (5).

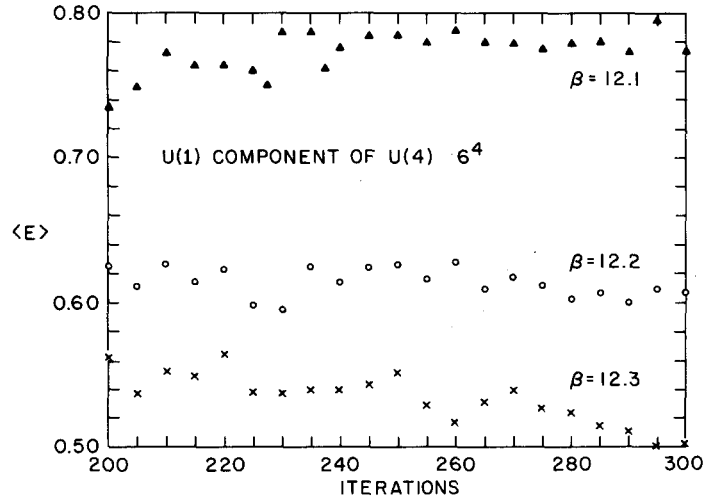

Fig. 7. The evolution of the average U(1) action per plaquette $\langle \bar{E} \rangle$ on a 6^4 lattice as a function of the number of iterations through the lattice for mixed phase starting lattices for various values of the inverse temperature β.

The string tension $\bar{\chi}(I, J)$, for $(I, J) = (1, 1)$, $(2, 2)$, $(3, 2)$ and $(3, 3)$, as a function of the inverse temperature β, is shown in fig. 9. The leading-order high-temperature expansion of eq. (5) is also indicated in fig. 9. If we compare the results of fig. 9 with those of fig. 4, we can see that in the low-temperature region the quantities $\bar{\chi}(I, J)$ decrease more rapidly with increasing rectangular dimensions I and J than is the case for the quantities $\chi(I, J)$. The data in the weak-coupling region are consistent with the area term in the quantity $\bar{\chi}(I, J)$ going to zero as the Wilson loop size goes to infinity. In consequence, the U(1) charges of U(4) gauge theory appear not to be confined in the low-temperature region as is the case with pure U(1) gauge theory [14, 15].

In fig. 10 we show the average action per plaquette $\langle E \rangle$, as a function of the inverse temperature on a 6^4 lattice, for pure SU(4) gauge theory. Our results in fig. 10 are in good agreement with the leading-order high- and low-temperature expansions of eqs. (1) and (3), respectively. In fig. 11 we show some of the mixed phase starting runs for the average action per plaquette in the neighborhood of the first-order phase transition of pure SU(4) gauge theory. This figure suggests a first-order phase transition at $\beta_c = 10.2 \pm 0.2$. The Wilson loops of size up to 3×3 are shown in fig. 12 as well as the leading-order high-temperature expansion of eq. (1) for comparison.

In figs. 13a, b we show the logarithmic ratios $\chi(I, J)$, for $(I, J) = (1, 1)$, $(2, 2)$, $(3, 2)$ and $(3, 3)$, for pure SU(4) gauge theory as a function of the inverse temperature β. We also show the leading-order high-temperature expansion of eq. (4) in fig. 13a. In fig. 13b we show the vicinity of the transition inverse temperature.

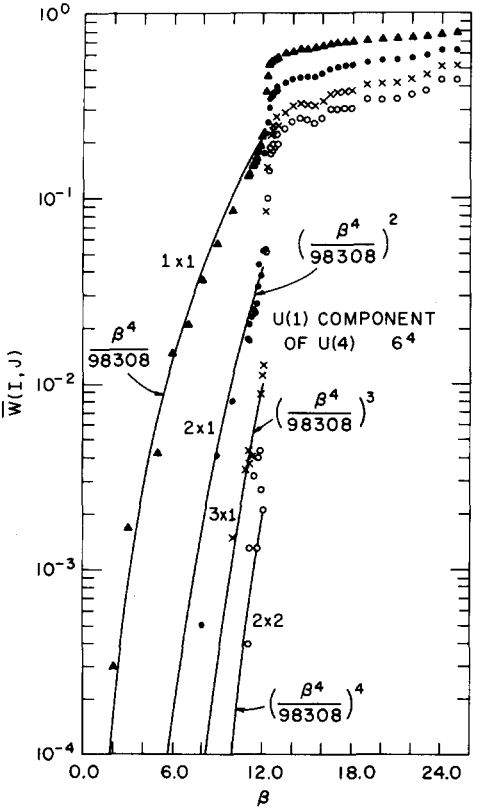

Fig. 8. The Wilson loops $\bar{W}(I, J)$ for the U(1) component of pure U(4) gauge theory on a 6^4 lattice as a function of the inverse temperature β. The full upward triangles represent $(I, J) = (1, 1)$, the full circles represent (2, 1), the crosses represent (3, 1), the open circles represent (2, 2). The curves represent the leading-order high-temperature expansion of eq. (5).

On these figures we show a band representing the weak-coupling 2-loop perturbative behavior, with $\Lambda_0 = (4.5 \pm 0.5) \times 10^{-3} \sqrt{K}$, where Λ_0 is the asymptotic freedom scale for the lattice cutoff and K is the physical string tension, as discussed in ref. [9].

Note that in fig. 13 the string tension appears nearly continuous from the weak-coupling to the strong-coupling regimes. Although a first-order transition would indicate a discontinuity, the size of the jump is rather small. SU(4) represents a borderline case, where the first-order transition present for large SU(N) just appears. We believe that the mixed phase runs shown in fig. 11 indicate the reality of the transition, but note the expanded scale in that figure relative to that in the U(4) case shown in fig. 2.

Our results are consistent with confinement of fundamental charges for couplings on either side of the SU(4) phase transition. Indeed, as emphasized in ref. [2], the mere existence of a transition in a lattice gauge theory does not necessarily imply

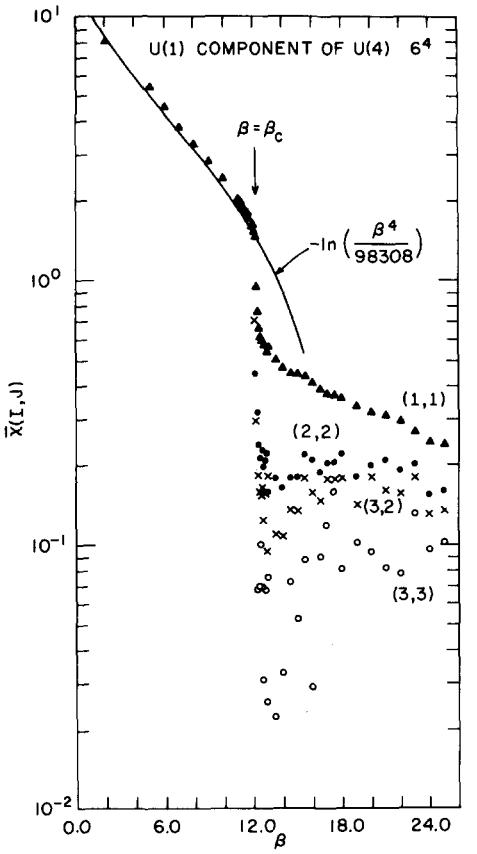

Fig. 9. The string tension $\bar{\chi}(I, J)$ for the U(1) component of pure U(4) gauge theory on a 6^4 lattice as a function of the inverse temperature β. The full upward triangles represent $(I, J) = (1, 1)$, the full circles represent (2, 2), the crosses represent (3, 2) and the open circles represent (3, 3). Also shown in the diagram is the leading-order high-temperature expansion of eq. (6).

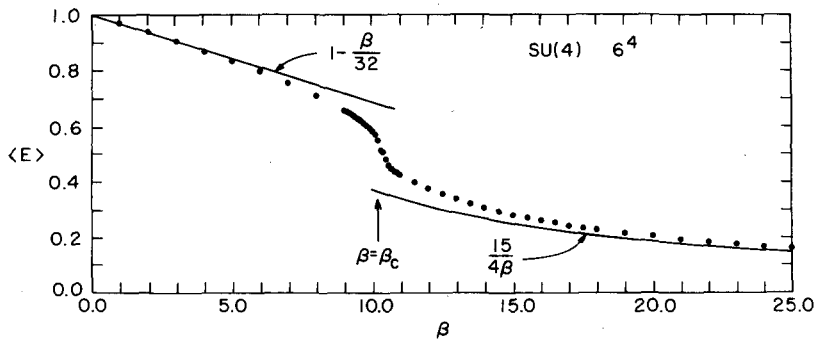

Fig. 10. The average action per plaquette $\langle E\rangle$ for pure SU(4) gauge theory on a 6^4 lattice as a function of the inverse temperature β. The curves represent the leading-order high- and low-temperature expansions of eqs. (1) and (3), respectively.

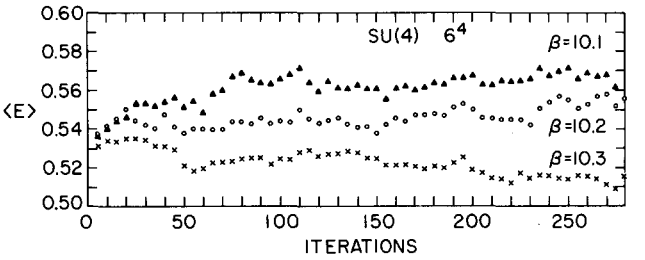

Fig. 11. The evolution of the average action per plaquette $\langle E \rangle$ for pure SU(4) gauge theory on a 6^4 lattice as a function of the number of iterations through the lattice for mixed phase starting lattices for various values of the inverse temperature β.

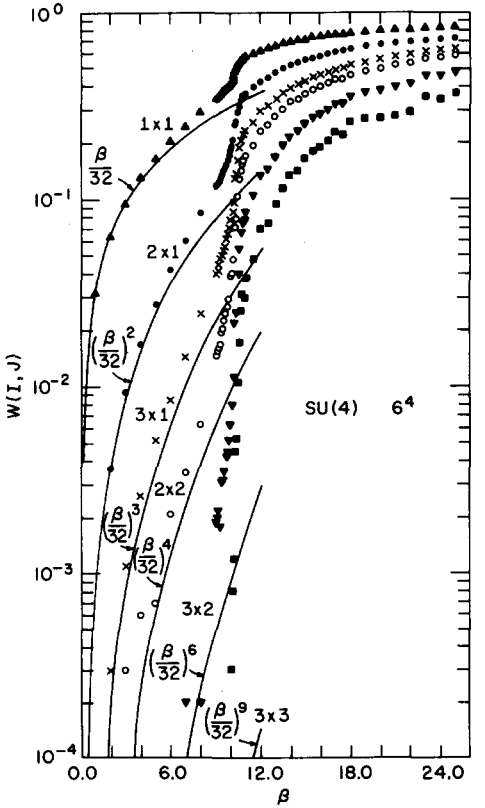

Fig. 12. The Wilson loops $W(I, J)$ for pure SU(4) gauge theory on a 6^4 lattiee as a function of the inverse temperature β. The full upward triangles represent $(I, J) = (1, 1)$, the full circles represent (2, 1), the crosses represent (2, 2), the full downward triangles represent (3, 2) and the full squares represent (3, 3). The curves represent the leading-order high-temperature expansion of eq. (1).

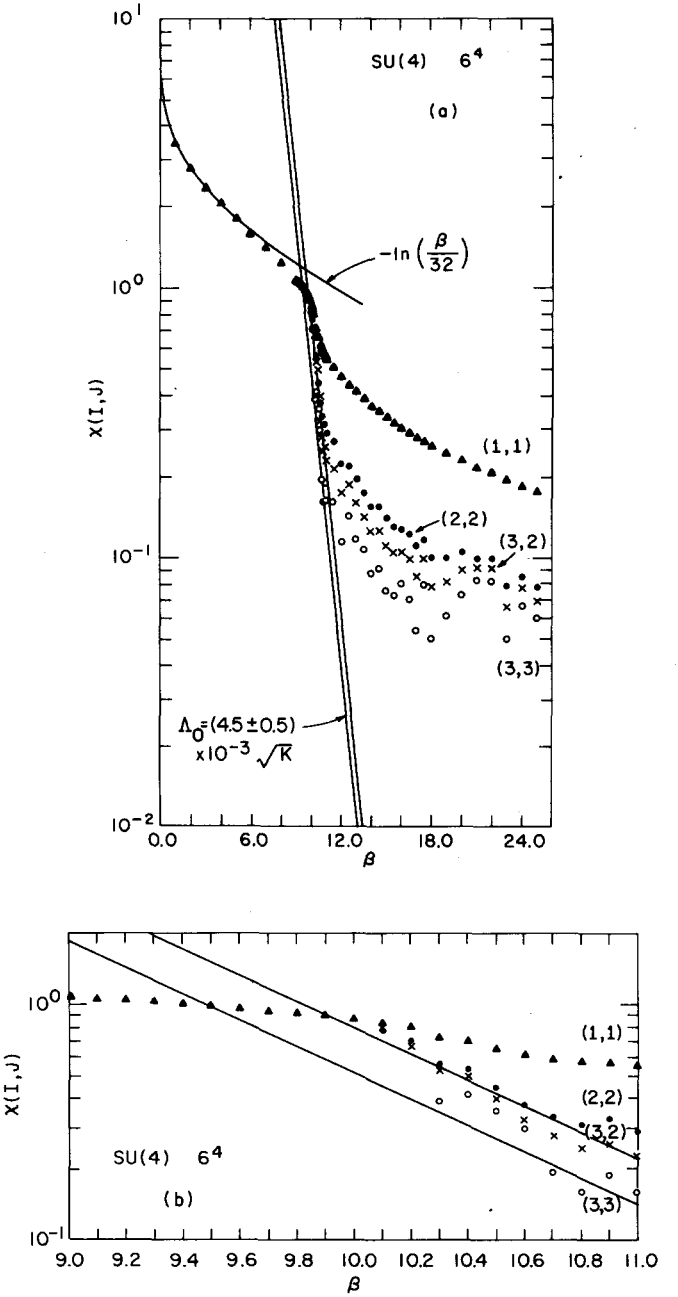

Fig. 13. The string tension $\chi(I, J)$ for pure SU(4) gauge theory on a 6^4 lattice as a function of the inverse temperature β. The full upward triangles represent $(I, J) = (1, 1)$, the full circles represent (2, 2), the crosses represent (3, 2) and the open circles represent (3, 3). Also shown in the diagram is the leading-order high-temperature expansion of eq. (4) and the asymptotic freedom scaling of the string tension with $\Lambda_0 = (4.5 \times 0.5) \times 10^{-3} \sqrt{K}$.

a loss of confinement. As we have no order parameter distinguishing the two SU(4) phases, it is possible that a generalization of the Wilson action may permit a smooth continuation between them.

In contrast, with the group U(4) we have the U(1) string tension to serve as an order parameter. This suggests that here the transition cannot be continued around without breaking the U(1) symmetry. It may, however, be possible to modify the action to convert the transition into a second-order one, as present in the pure U(1) theory. These questions are currently under investigation.

We would like to thank the Science and Engineering Research Council of Great Britain for the award of research grants (grants NG-0983.9 and NG-1068.2) to buy time on the CRAY-1S computer at Daresbury Laboratory where part of this calculation was carried out, the University of London Computer Centre for the granting of discretionary time on their CRAY-1S where another part of this calculation was performed and the Control Data Corporation for the award of a research grant (Grant 82CSU13) and the Institute for Computational Studies at Colorado State University for the granting of time on their CDC CYBER 205 where the remainder of this calculation was performed. The calculations of the present paper took the equivalent of 147 CDC 7600 hours to perform. One of the authors (KJMM) wishes to thank the CERN directorate for the award of a Scientific Associateship to visit CERN where this work was completed. This research was also carried out in part under the auspices of the US Department of Energy under contract no. DE-AC02-76CH00016.

References

[1] M. Creutz and K.J.M. Moriarty, Phys. Rev. D25 (1982) 610
[2] M. Creutz, Phys. Rev. Lett. 46 (1981) 1441;
K.J.M. Moriarty, Phys. Lett. 106B (1981) 130
[3] M. Creutz and K.J.M. Moriarty, Nucl. Phys. B210 [FS6] (1982) 59
[4] M. Creutz, Phys. Rev. D21 (1980) 2308
[5] M. Creutz and K.J.M. Moriarty, Nucl. Phys. B210 [FS6] (1982) 377
[6] M. Creutz and K.J.M. Moriarty, Phys. Rev. D26 (1982) 2166
[7] K.G. Wilson, Phys. Rev. D10 (1974) 2445
[8] N. Metropolis, A.W. Rosenbluth, M.N. Rosenbluth, A.H. Teller and E. Teller, J. Chem. Phys. 21 (1953) 1087
[9] M. Creutz, 1981 Erice Lectures
[10] R.W.B. Ardill, M. Creutz and K.J.M. Moriarty, Compt. Phys. Comm. 29 (1983) 000
[11] F. Green and S. Samuel, Phys. Lett. 103B, 48 (1981);
S. Samuel, Calculating the large-N phase transitions in lattice gauge theories, Columbia University Preprint, CU-TP-216, October 1981, and references therein
[12] D. Barkai and K.J.M. Moriarty, Compt. Phys. Comm. 27 (1982) 105
[13] M. Creutz, L. Jacobs and C. Rebbi, Phys. Rev. Lett. 42 (1979) 1390
[14] B. Lautrup and M. Nauenberg, Phys. Lett. 95B (1980) 63;
T.A. Degrand and D. Toussaint, Phys. Rev. D24 (1981) 466;
K.J.M. Moriarty, Phys. Rev. D25 (1982) 2185
[15] K.J.M. Moriarty, J. Phys. G9 (1983) L33